BMC Veterinary Research

RESEARCH

Open Access

# Developing a PK-PD model for propofol in exhaled air and the BIS following fospropofol disodium in beagles

Xiaoxiao Li[1,2†], Pan Chang[1,2†], Xing Liu[1,2], Yi Kang[1,2], Zhongjun Zhao[3], Yixiang Duan[3] and Wensheng Zhang[1,2*]

## Abstract

**Background** Fospropofol, a water-soluble prodrug of propofol, is metabolized into propofol by alkaline phosphatase after administration. This study aimed to develop a pharmacokinetic-pharmacodynamic (PK-PD) model that correlates the propofol concentration in exhaled air (Ce-pro-f) with its anesthetic effects, as measured by the bispectral index (BIS) in beagles.

**Methods** Beagles receiving a single intravenous infusion of fospropofol at varying doses were divided into three groups ($n=6$): the DBL-fospro group (15 mg/kg), the DBM-fospro group (30 mg/kg), and the DBH-fospro group (60 mg/kg). Propofol levels were monitored using VUV-TOF MS from pre-administration to recovery. Correlations between Ce-pro-f and blood concentration ($C_{blood}$-pro), as well as between Ce-pro-f and the BIS were investigated. PK, PD, and PK-PD models describing the relationship between Ce and BIS were also analyzed.

**Results** Propofol concentration in exhaled air can be quantified using VUV-TOF MS at a mass-to-charge ratio of 177.6. After fospropofol injection, the peak Ce-pro-f was delayed compared to $C_{blood}$-pro. The PK model of Ce-pro-f can be described using a noncompartmental approach, corresponding to the linear PK characteristics. Additionally, Ce-pro-f showed a moderate to strong negative correlation with BIS values. In the PK-PD model, the PK component was well characterized by a two-compartment model incorporating a first-order delay to account for the time lag of Ce-pro-f relative to $C_{blood}$-pro. The PD component was well fitted by the inhibitory sigmoid $E_{max}$ model, with an indirect connection model selected to explain the observed lag between BIS signals and Ce-pro-f peaks.

**Conclusions** This study is the first to develop a PK-PD model for exhaled propofol in beagles after fospropofol disodium administration. The PK profile was described by a two-compartment model with a first-order delay, and the PD profile was modeled using an inhibitory sigmoid $E_{max}$ model with an indirect connection model to capture the lag between BIS and exhaled propofol peaks.

**Keywords** Exhaled air, Propofol, Fospropofol, VUV-TOF MS, PK-PD model

†Xiaoxiao Li and Pan Chang contributed equally to this work.

*Correspondence:
Wensheng Zhang
zhang_ws@scu.edu.cn
[1]Department of Anesthesiology, West China Hospital, Sichuan University, Chengdu, Sichuan, China
[2]Laboratory of Anesthesia and Critical Care Medicine, West China Hospital, National-Local Joint Engineering Research Centre of Translational Medicine of Anesthesiology, Sichuan University, Chengdu, Sichuan, China
[3]School of Mechanical Engineering, Sichuan University, Chengdu, Sichuan, China

## Introduction

Fospropofol disodium, the prodrug of propofol, produces sedative effects through its metabolic conversion into propofol by alkaline phosphatase. Its water solubility markedly reduces injection pain commonly associated with lipid emulsion. However, hypotension at high concentrations remains similar to that of propofol, emphasizing the need for individualized monitoring of drug levels. Developing a pharmacokinetic (PK) and pharmacodynamic (PD) model based on propofol can optimize fospropofol disodium dosing, minimize overdose-related adverse effects [1], and support the development of closed-loop drug delivery systems [2, 3].

Traditional PK modeling involves invasive blood sampling and repeated collections. The requirement for multiple sampling points prolongs analysis time and increases costs, while also increasing patient discomfort and the risk of puncture site infections. More critically, the inability to perform continuous, large-scale real-time blood sampling limits the reliability and accuracy of the established models, which may fail to accurately reflect individual pharmacokinetic variability [4–6]. Therefore, developing a simple, noninvasive method for real-time online analysis of drug concentrations is crucial [7]. Recent studies have confirmed that propofol can be eliminated through the respiratory system, and with advanced analytical technologies such as proton transfer reaction mass spectrometry (PTR-MS), selected ion flow tube mass spectrometry (SIFT-MS), and ion mobility spectrometry (IMS), propofol has be successfully detected in exhaled air [8–10]. However, research on PK-PD models correlating exhaled propofol concentrations with anesthesia depth monitoring is still in the early stage.

Our team has developed an exhaled air analyzer using vacuum ultraviolet photoionization combined with time-of-flight mass spectrometry (VUV-TOF MS). Preliminary studies in rats and beagles have demonstrated the successful detection of propofol and ciprofol in exhaled air, enabling the establishment and validation of a gas analysis methodology for these anesthetic agents [11–13]. Beagles were selected as the research subjects in this study due to their physiological structure and metabolic pathways being similar to those of humans, effectively simulating human pharmacokinetics in drug absorption, distribution, metabolism, and excretion. Single intravenous doses of fospropofol disodium at varying levels were administered to beagles to investigate the changes in exhaled propofol concentrations (Ce-pro-f), their correlation with blood drug levels ($C_{blood}$-pro), and their relationship with anesthesia depths as indicated by the bispectral index (BIS). The aim was to establish a PK-PD model linking Ce-pro-f with BIS, providing novel insights and data support for future PK studies utilizing exhaled air analysis.

## Materials and methods

### System design of VUV-TOF MS

The VUV-TOF MS, with dimensions of 0.59 m*0.59 m*0.94 m, is equipped with casters for easy mobility. Its core components include a VUV photoionization source, a radio-frequency multirod ion transmission system, electrostatic lenses, and a reflectron TOF MS. The VUV photoionization source emits 10.6 eV photons, enabling rapid and soft ionization of volatile organic compounds (VOCs) in gas samples without the need for prior sample preparation. The reflectron TOF MS, featuring a 265 mm flight tube and operating at 2400 V, comprises an accelerator, a field-free flight area, a reflector, and a microchannel plate detector. By integrating VUV photoionization with high-sensitivity TOF MS, this system facilitates rapid response times and real-time acquisition of high-resolution, full-scan spectral data from exhaled air. The VUV-TOF MS allows for the sensitive detection of VOCs at concentrations as low as parts per billion by volume (ppbv) and even parts per trillion by volume (pptv), supporting high-throughput, precise, and rapid online quantification of trace VOCs in exhaled air.

### Calibration of the VUV-TOF MS

A custom-designed gas generator was used for calibration. The structure, operation process, and calibration method of the gas generator has been described in detail in previous studies [11–13]. Given the insolubility of propofol in water, liquid propofol standards were first dissolved in methanol, and then diluted with water [14]. The room temperature was maintained at 25 °C. To prepare the stock solution, 20 μL of the propofol standard solution, 8 mL of chromatographic-grade methanol and 42 mL of pure water were thoroughly mixed. Using the ideal gas equation $pV = nRT$, the concentration of propofol gas ($C_0$) after vaporization was calculated. Stand standard dilution solutions were then prepared by mixing various proportions of the stock solution with pure water to obtain 50 mL solutions at concentrations of 1.56 ppbv, 15.56 ppbv, 77.82 ppbv, 108.95 ppbv, 155.65 ppbv, 233.47 ppbv, 311.30 ppbv, 466.95 ppbv, 778.25 ppbv, and 1556.49 ppbv. By adjusting the concentration of the propofol solution in the gas generator channel and the flow rate of $N_2$, standard propofol gases were generated at concentrations ranging from 0.04 ppbv to 55.68 ppbv.

The VUV-TOF MS conditions were optimized as follows: high-purity $N_2$ was used as the carrier gas at a flow rate of 70 mL/min; the UV ion source and sample tube temperature was set to 100 °C, and the pulse interval was 50 μs with 400,000 accumulations, resulting in a 20-second analysis interval (single data acquisition time = number of accumulations * pulse interval). Before each use, the UV ion source and sample tube were preheated for 1 h.

## Experimental methods

### Animals

Six male beagles, aged 1-1.5 years and weighing between 10 and 14 kg were selected as research subjects. The animals were obtained from Chengdu Dossy Experimental Animal Co., Ltd. All beagles underwent blood biochemical testing, and those with significant abnormal results were excluded from the study. Prior to the experiments, the beagles were provided with free access to food and water following a one-week environmental acclimatization period. Ethical approval was granted by the Animal Ethics Committee of West China Hospital, Sichuan University (20211022), and all procedures adhered to animal welfare regulations. This methods section was described in accordance with the ARRIVE reporting guidelines.

### Administration method and dosage

The sample size was determined based on the "Guiding Principles for Registration Review of Animal Testing in Medical Device Studies" issued in China, as well as the requirements of pharmacological experiments. Therefore, each group consisted of six beagles [15]. Using the random number table method, six beagles were randomly assigned to receive three different doses of fospropofol disodium (50 mg/mL, Yichang Humanwell, Wuhan, China) in a crossover design: a low dose (DBL-fospro group, 15 mg/kg), a medium dose (DBM-fospro group, 30 mg/kg), and a high dose (DBH-fospro group, 60 mg/kg). Each beagle received all three dosing levels with a 7-day washout period between administrations. The dosing regimen was determined based on the median effective dose ($ED_{50}$) required to induce the loss of the righting reflex in beagles, derived from data generated by our research center. Each dose was administered at a constant rate of 720 mL/h (0.2 mL/s) using a calibrated micro-infusion pump. This process was blinded to the personnel responsible for outcome assessment.

### Beagle ventilation model preparation

All beagles were fasted for 12 h prior to the experiment but had free access to water. Upon entering the procedure room, bilateral forearm venous catheterization was performed. The 22 G intravenous catheter (Surflo Flash, Terumo, Japan) was inserted into the cephalic veins of both forelimbs. The right cephalic vein was utilized for drug administration, whereas the left was utilized for blood sampling. Anesthesia was induced by intravenous administration of 5 mg/kg Zoletil 50 via the forearm vein, with supplemental doses administered as needed. Following the loss of the righting reflex, the beagles were positioned on a heated, constant-temperature experimental table and connected to a vital signs monitor to track heart rate (HR), electrocardiography (ECG), pulse oxygen saturation ($SpO_2$), and invasive blood pressure. Once muscles relaxation and regular breathing were achieved, tracheal intubation was performed, and the beagles were connected to a ventilator. The ventilator settings included volume-controlled ventilation mode, pure oxygen at a flow rate of 2 L/min, a respiratory rate of 20 breaths/min, and a tidal volume of 10 mL/kg. Prior to drug administration, the end-tidal carbon dioxide partial pressure ($P_{ET}CO_2$) was maintained between 25 and 45 mmHg, with ventilator parameters adjusted only if $P_{ET}CO_2$ was $<25$ mmHg or $>45$ mmHg. BIS electrodes were placed on the foreheads of the beagles to monitor anesthesia depth, and intraoperative body temperature was maintained at $36.5 \pm 0.5$ °C. Postoperatively, tracheal tubes were removed once the beagles regained consciousness, defined as persistent, severe coughing and active attempts to dislodge the tube.

### Exhaled air sampling and analysis

The L-shaped adapter of the respiratory circuit was directly connected to the sampling inlet of the VUV-TOF MS via a three-way valve, enabling continuous collection of exhaled air. As described previously, the mass spectrometry conditions were set to a sampling rate of 70 mL/min with an analysis interval of 20 s. Exhaled air was collected from 3 min prior to the start of drug infusion until the beagles regained consciousness.

### Blood sampling and analysis method

Blood samples were collected at baseline (0 min), 1 min, 3 min, 5 min, 7 min, 10 min, and 20 min after drug infusion (if applicable), at subsequent 10-minute intervals (e.g., 30–40 min, if applicable), and at the time of awakening. 0.2 mL of venous blood was drawn from the left cephalic vein at each time points. From this, 50 µL was precisely transferred into an EP tube containing 350 µL of methanol to deactivate alkaline phosphatase. The mixture was centrifugated at 20,000 rpm for 10 min at 4 °C to obtain the supernatant. The processed samples were then transferred to labeled EP tubes and stored at -80 °C until analysis.

High-performance liquid chromatography (HPLC) was employed for propofol concentration analysis: chromatographic column: Swell Chromplus C18 (150 mm × 4.6 mm, 5 µm); column temperature: 30 °C; mobile phase: pure water: acetonitrile (38:62, v/v); fluorescence wavelength: excitation wavelength 276 nm, emission wavelength 310 nm; flow rate: 1.0 mL/min; injection volume: 10 µL; retention times: vanillin (internal standard): 3.9 min, and propofol: 7.4 min.

Detailed information on the methodology for the quantitative detection of fospropofol disodium in whole blood ($C_{blood}$-fospro) is provided in the Supplementary Material 1.

#### *Anesthesia depth monitoring*

In previous animal studies, the BIS has been widely used to assess anesthesia depth [16, 17], with research demonstrating a strong correlation between BIS and anesthesia depth in most cases [18]. The baseline BIS value was calculated as the average of five consecutive measurements taken prior to drug administration. Data were collected from the start of drug administration until the time of awakening, with measurements recorded at 20-second intervals.

#### Statistical analysis, PK and PD modeling

Statistical analysis was performed using IBM SPSS software version 22.0. The Shapiro-Wilk test was used to assess the normality of the data. Quantitative data were expressed as the mean ± standard deviation or median (interquartile range). For normally distributed data, one-way ANOVA was used; For nonnormally distributed data, the Kruskal-Wallis rank-sum test was used. Spearman's rank analysis was used to calculate correlations between drug concentrations:$|r| = 0.8–1.0$ indicated an extremely strong correlation;$|r| = 0.6–0.8$ indicated a strong correlation;$|r| = 0.4–0.6$ indicated a moderate correlation;$|r| = 0.2–0.4$ indicated a weak correlation;$|r| = 0.0–0.2$ indicated no correlation.

When establishing a regression equation between drug concentrations, scatter plots are first drawn to determine the linear or curvilinear relationships, followed by fitting using a linear or single exponential combined model equation. $Y_0$, Plateau, and K are the model parameters. The least squares method was used to estimate the best model parameters and calculate $R^2$, with a higher $R^2$ indicating a better fit.

$$\mathrm{Y} = \mathrm{Y0} + (\mathrm{Plateau} - \mathrm{Y0}) * (1 - \mathrm{e} - \mathrm{K}*\mathrm{X})$$

The PK and PD analyses were conducted using Phoenix WinNonlin software. The noncompartmental analysis (NCA) module was used for PK modeling. Concentrations below the limit of quantification were considered zero before reaching the maximum concentration ($C_{max}$) and were considered unquantifiable after reaching $C_{max}$.

The PD modeling was based on the BIS as the measure of drug effect and exhaled propofol concentrations as the exposure variable, with data fitted using the inhibitory sigmoid $E_{max}$ model. If the coefficient of variation (CV) was less than 20%, the precision of the model's estimated parameters was considered appropriate.

$$\text{Inhibitory sigmoid } \mathrm{E_{max}} \text{ model}: \ \mathrm{E} = \mathrm{E0} - \frac{\mathrm{E_{max}}*\mathrm{C}^{\gamma}}{\mathrm{IC}_{50}^{\gamma} + \mathrm{C}^{\gamma}}$$

Data trends were interpreted using combined PK-PD models; direct connection models were applied to data where BIS changes showed no substantial lag compared to Ce; indirect connection models, incorporating the effect compartment equilibration rate constant ($K_{e0}$), were used for data where BIS changes lagged significantly behind Ce. Differences were considered statistically significant at $P < 0.05$.

## Results

#### Biochemical indexes of the beagles

Table 1 describes the biochemical indexes of the selected 6 beagles, which were all within normal ranges. All baseline measurements for the relevant indexes were conducted before the first drug administration.

#### Calibration of propofol in exhaled air

The spectrum of propofol gas shows that the signal intensity is strongest at a mass-to-charge ratio (m/z) = 177.6. The spectral analysis of the blank and drug-containing exhaled air samples indicated that endogenous VOCs in the exhaled air of the beagle did not interfere with the propofol measurement (Fig. 1a and b). When the propofol concentration ranged from 0.04 ppbv to 50.29 ppbv, the signal intensity at m/z = 177.6 showed a curvilinear relationship with the gas concentration: $y = -142 + 23{,}562*x + 1461*x^2$ ($R^2 = 0.9992$) (Fig. 1c), and the model passed the lack-of-fit test ($P = 0.36$). However, the linear fit showed a poor correlation: $y = -258{,}412 + 83{,}944*x$ ($R^2 = 0.9197$, $P < 0.05$) (Fig. 1d). In this study, we performed calibration using the curvilinear equation from Fig. 1c. Based on a signal-to-noise ratio of

**Table 1** The basic biochemical indexes of beagles

| | Beagle #1 | Beagle #2 | Beagle #3 | Beagle #4 | Beagle #5 | Beagle #6 |
|---|---|---|---|---|---|---|
| ALT, U/L | 21.72 | 47.13 | 61.18 | 27.45 | 36.43 | 36.82 |
| AST, U/L | 29.11 | 29.04 | 33.77 | 24.73 | 29.82 | 41.01 |
| CK-MB, U/L | 627.91 | 505.76 | 524.06 | 495.85 | 1019.47 | 865.25 |
| CREA, μmol/L | 125.20 | 124.63 | 109.11 | 142.27 | 137.89 | 255.37 |
| LDH, U/L | 137.83 | 98.22 | 123.26 | 109.83 | 195.10 | 159.27 |
| TG, mmol/L | 0.39 | 0.48 | 0.42 | 0.43 | 0.52 | 0.44 |
| UREA, mmol/L | 5.20 | 6.61 | 5.64 | 7.35 | 4.62 | 5.66 |

*Notes* ALT, alanine aminotransferase; AST, glutamic oxalacetic transaminase; CK-MB, creatine kinase-MB; CREA, creatinine; LDH, lactate dehydrogenase; TG, triglyceride; UREA, urea nitrogen. All baseline measurements were conducted before the first administration

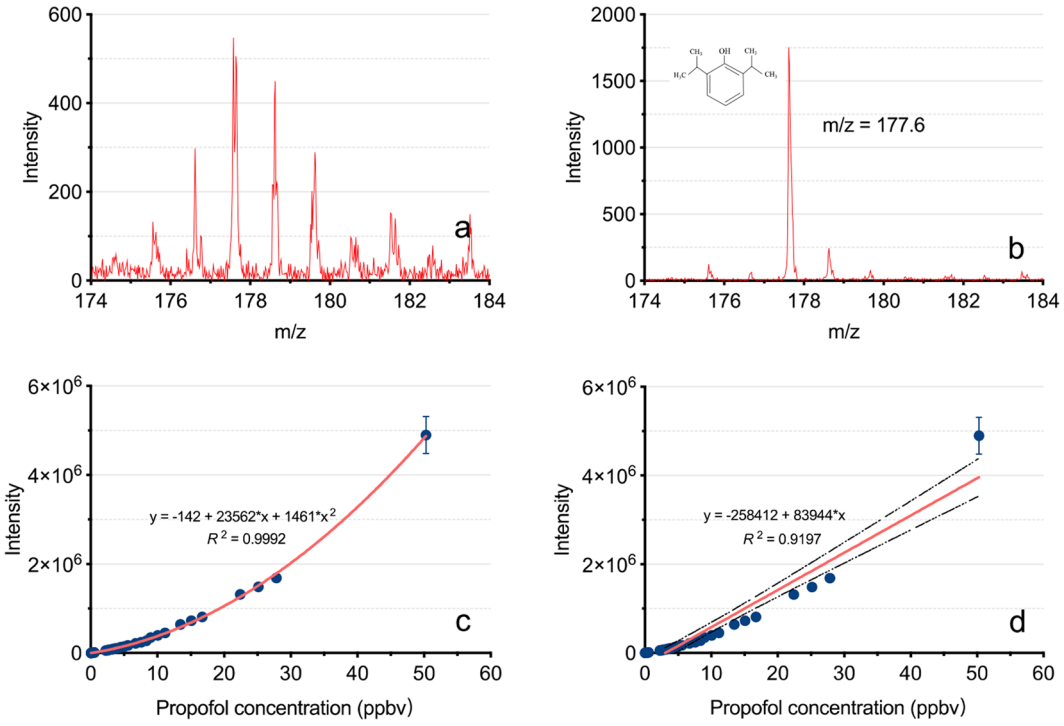


**Fig. 1** Calibration plot of propofol based on VUV-TOF MS. **a**. shows the spectrum of blank exhaled air from beagles; **b**. shows the spectrum of propofol-containing exhaled air from beagles; **c**. shows the curvilinear fitting of the calibration curve; **d**. shows the linear fitting of the calibration curve.

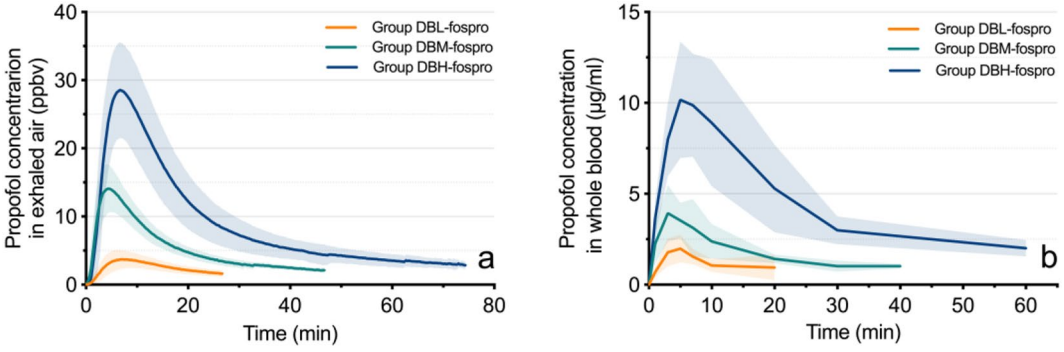


**Fig. 2** Concentration-time curves of the propofol concentration in exhaled air and in whole blood. (**a**) and (**b**) show the concentration-time curves of the propofol concentration in exhaled air and in whole blood after injecting fospropofol disodium, respectively

3:1, the limit of detection is 0.04 ppbv; with a signal-to-noise ratio of 10:1, the limit of quantification is 0.12 ppbv.

### PK parameters of Ce-pro-f

The PK models for Ce-pro-f were well fitted using the NCA approach (detailed parameters are provided in Supplemental Table S1). After intravenous administration of low, medium, or high doses of fospropofol disodium, $C_{blood}$-fospro peaked rapidly at 1 min (Supplemental Fig. S1). As shown in Fig. 2a and b, the peak time for $C_{blood}$-pro was slightly later (DBL-fospro group: 4.33 ± 1.03 min; DBM-fospro group: 4.00 ± 1.67 min; DBH-fospro group: 5.33 ± 0.61 min). In comparison, the time to peak Ce-pro-f was further delayed (DBL-fospro group: 7.25 ± 1.71 min; DBM-fospro group: 4.33 ± 0.82 min; DBH-fospro group: 6.67 ± 0.82 min). The $C_{max}$ of Ce-pro-f (DBL-fospro group: 4.00 ± 1.68 ppbv; DBM-fospro group: 14.23 ± 3.69 ppbv; DBH-fospro group: 28.83 ± 7.06 ppbv) increased linearly with the administered dose ($P = 0.04$), and the $AUC_{0-\infty}$ values (DBL-fospro group: 114.55 ± 48.77 min*ppbv; DBM-fospro group: 307.96 ± 65.69 min*ppbv; DBH-fospro group: 750.22 ± 243.96 min*ppbv) also showed a linear dose-response relationship ($P = 0.02$). Additionally, the elimination half-life was independent of the dose ($P = 0.24$), indicating linear PK characteristics.

### Correlations between Ce-pro-f, Cblood-pro, and BIS

Spearman analysis revealed significant moderate to strong correlations between Ce-pro-f and $C_{blood}$-pro following a single intravenous infusion. The correlation coefficients were as follows: DBL-fospro group, $r = 0.55$ ($P < 0.001$); DBM-fospro group, $r = 0.73$ ($P < 0.001$); and DBH-fospro group, $r = 0.79$ ($P < 0.001$). Figure 3a presents the BIS-time curves following the administration of three different doses of fospropofol disodium. Ce-pro-f showed moderate to strong negative correlations with BIS values after administration of different doses: $r$ = -0.47 ($P = 0.02$) in the DBL-fospro group (Fig. 3b); $r$ = -0.50 ($P = 0.004$) in the DBM-fospro group (Fig. 3c); and $r$ = -0.85 ($P < 0.001$) in the DBH-fospro group (Fig. 3d).

### PD models of Ce-pro-f and BIS

As shown in Fig. 4a and b, and 4c, the change in BIS values was significantly delayed compared to the changes in Ce-pro-f. This delay necessitates the introduction of a time correction to account for the lag between propofol concentrations in exhaled air and at the effect site, enabling the establishment of a more accurate PD model with BIS.

### The PK-PD model of Ce-pro-f with BIS

As shown in Fig. 5, after a single intravenous infusion of low, medium and high doses of fospropofol disodium, a delay in the Ce-pro-f was observed compared with $C_{blood}$-pro. However, BIS values exhibited an even greater delay relative to Ce-pro-f. To account for this, an indirect connection model was applied to the PK-PD model to capture the delayed pharmacodynamic response. The PK component was fitted using a two-compartment model, incorporating a first-order rate constant to describe the delay in equilibrium between the blood and the lung compartment ($Ke0_{lung}$). For the PD component, an inhibitory sigmoid $E_{max}$ model was employed to accurately capture the trend of BIS responses across all dose groups. The parameters of the established PK-PD model are presented in Supplemental Table S2.

### Ce-pro-f upon awakening

After a single intravenous infusion of low, medium or high doses of fospropofol disodium, the anesthesia times were 26.67 ± 7.55 min, 46.67 ± 7.57 min, and 74.34 ± 10.97 min, respectively. The Ce-pro-f upon awakening were 1.34 ± 0.18 ppbv, 2.01 ± 1.00 ppbv, and 2.59 ± 0.60 ppbv, respectively ($P = 0.02$), suggesting that Ce-pro-f increased with increasing dosage.

## Discussion

Our study revealed a moderate to strong correlation between the Ce-pro-f and $C_{blood}$-pro in beagles administered fospropofol disodium, along with its anesthetic effects as indicated by the BIS. Furthermore, this study established PK, PD, and PK-PD models based on the

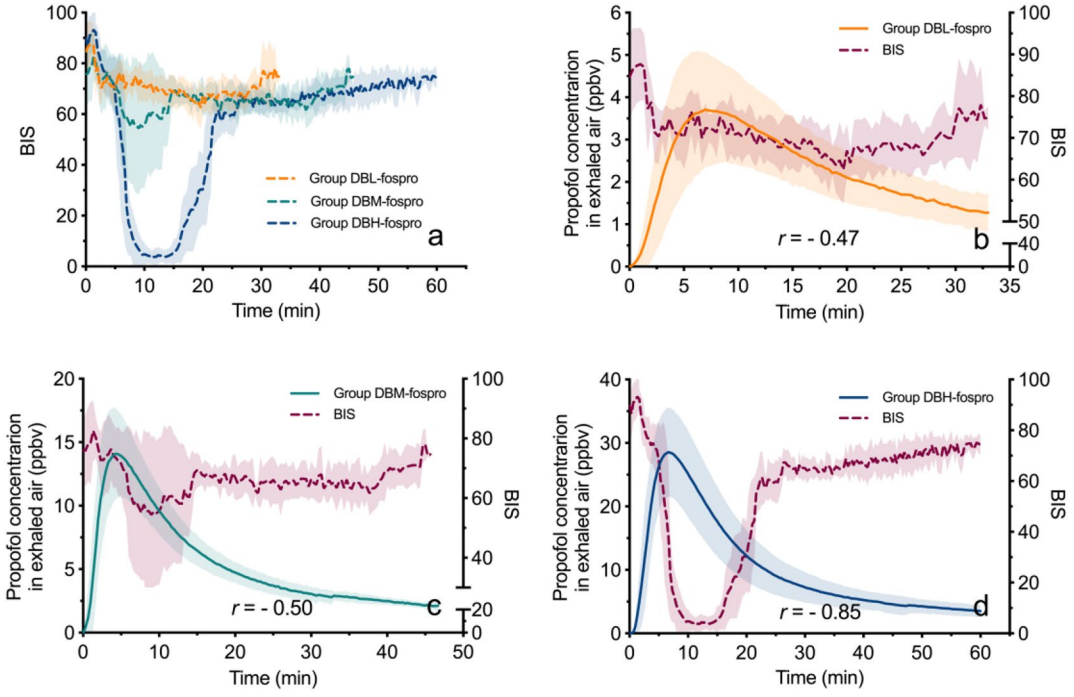


**Fig. 3** Correlations between the propofol concentration in exhaled air and BIS (**a**) presents the BIS-time curves following the administration of three doses of fospropofol disodium; (**b**), (**c**), and (**d**) depict the correlations of propofol concentration in exhaled air and BIS under single intravenous infusion of low, medium, and high doses of fospropofol disodium, respectively

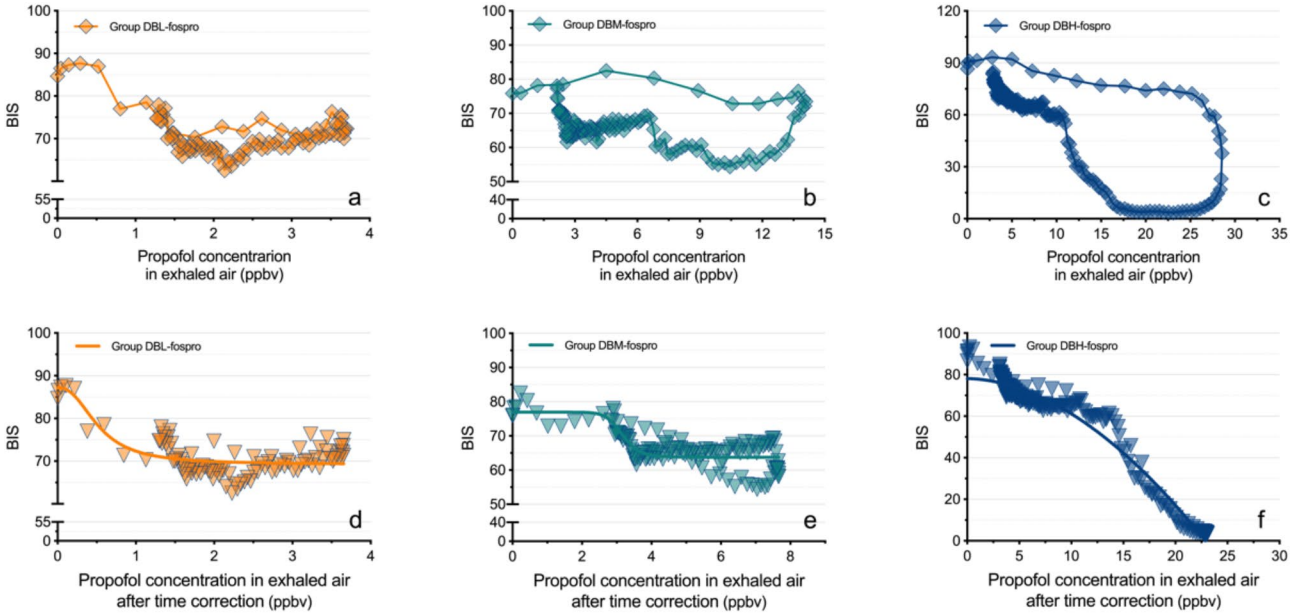


**Fig. 4** PD models of propofol concentration in exhaled air and BIS (**a**), (**b**), and (**c**) are the curves of propofol concentration in exhaled air and BIS; (**d**), (**e**), and (**f**) are the time-corrected curves of propofol concentration in exhaled air and BIS

Ce-pro-f and BIS, providing significant support for future PK/PD studies on fospropofol disodium.

Real-time monitoring of drug concentrations allows for timely data acquisition, enabling the accurate determination of PK/PD model parameters. This approach helps improve traditional PK-PD models, optimizes dosing regimens, and supports the development of personalized treatment strategies [7]. Compared to traditional offline plasma sampling, this study utilizes VUV-TOF MS for real-time analysis of exhaled air, clearly visualizing the changes in exhaled propofol concentration after administrating fospropofol disodium in beagles. The findings align with those of previous studies [19–21]. The appearance of propofol molecules in exhaled air occurs as follows: after intravenous infusion, propofol rapidly distributes to the lungs. As blood carrying propofol passed through the alveoli, unbound propofol volatilizes to form headspace gas, which crosses the pulmonary respiratory membrane, enabling the transfer of propofol molecules from the bloodstream to the alveoli. Although some studies suggest the airways may contribute to gas exchange, propofol- a lipophilic, hydrophobic drug with high blood solubility-is generally believed to primarily undergo gas exchange in the alveoli [22, 23].

Analyzing the structural features and parameters of PK and PD models enhancing the understanding of fundamental drug physiological processes. Propofol, the active metabolite of fospropofol disodium is believed to follow a three-compartment distribution model in pharmacokinetics. The PK model consists of a central compartment connected to both rapid and slow peripheral compartments [24–26]. Due to the sampling design omitting the full elimination phase, different PK models may emerge when applying compartmental models [27]. Therefore, a NCA approach was used for the PK calculations. Based on the NCA approach, we found that the elimination half-life of propofol in exhaled air from beagles remains constant regardless of the dosage administered. Additionally, both the peak concentration and the area under the curve show strong correlations with the administered dosage, indicating that changes in exhaled propofol follow linear PK behavior, similar to blood propofol levels. This further supports the potential application of gaseous drug concentrations in PK studies [28].

Compared to blood drug concentrations, the peak times of fospropofol disodium (active metabolite - propofol) in exhaled air are delayed. However, in vitro studies demonstrated that propofol spectral peaks are detectable in subsequent measurements when standard gas is introduced into the VUV-TOF MS system. This suggests that the delay is not due to tube adsorption but rather high plasma protein binding, which reduces the excretion of free drug molecules through the lungs [29, 30]. Additionally, the delay may result from propofol's large blood-to-gas partition coefficient; a higher coefficient slows the exchange of volatile substances between gas phases and liquid phases, prolonging the equilibrium between free drug molecules in the blood and the headspace gas. Propofol's high blood-gas partition coefficient suggests that its equilibrium occurs significantly later than that of other general anesthetics [31]. Grossherr et al. used IMR-MS to compare the clearance kinetics and peak

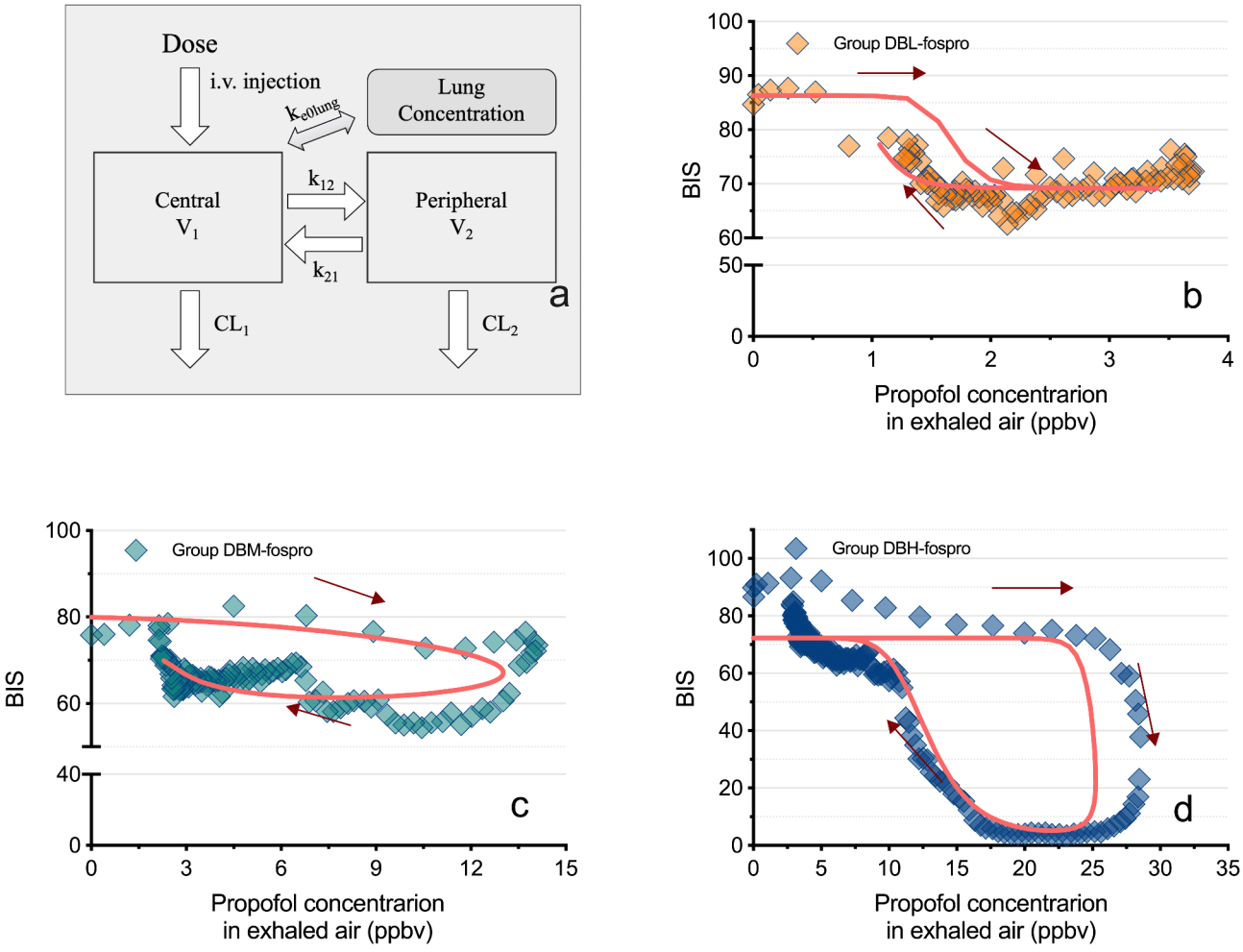


**Fig. 5** PK-PD models of propofol concentration in exhaled air and BIS (**a**). The schematic diagram of the PK-PD model. (**b**), (**c**), and (**d**) show the PK-PD models of propofol concentration in exhaled air and BIS at low, medium and high dosages of fospropofol disodium, respectively. $Ke0_{lung}$: a first-order rate constant to describe the delay in equilibrium between the blood and the lung compartment; $CL_1$: clearance rate in the central compartment; $CL_2$: clearance rate in the peripheral compartment

concentrations of ethanol and propofol in pig exhaled air, revealing that ethanol appeared and peaked much faster than propofol. This difference is due to factors like molecular weight, solubility, blood-gas partition coefficient, plasma protein binding, and lipophilicity. Propofol's larger molecular weight, higher blood-gas partition coefficient, and stronger protein binding contribute to its slower kinetics and delayed peak concentrations [32]. Correlations between gaseous and blood drug concentrations are crucial for their use in PK studies. In the fospropofol groups, all concentration-time curves showed moderate to strong correlations, allowing anesthesiologists to effectively monitor drug concentrations in real time. In PD modeling of blood propofol concentrations with BIS, incorporating the effect-compartment concentration is crucial to address the delayed equilibrium between BIS and blood levels. From our preliminary studies, the delay in exhaled propofol concentrations permits a direct substitution with effect-compartment concentrations in the PD model. For fospropofol disodium, although gaseous propofol concentrations are closer to effect- compartment levels than blood concentrations, a significant delay remains due to its conversion to propofol by alkaline phosphatase.

Furthermore, the PK-PD models developed in this study demonstrated that in the PK part, a delay exists in the equilibrium of propofol between the blood and the pulmonary compartment. To account for this delay, the parameter $Ke0_{lung}$ was introduced based on the model described by Kreuer et al., representing the first-order rate constant governing the equilibrium between blood and lung concentrations [20]. Meanwhile, a two-compartment model was employed, with the blood as the central compartment, and the lung as the peripheral compartment, effectively modeling the distribution and elimination processes. This approach allows for a more

accurate characterization of the delayed pharmacokinetic behavior of propofol in exhaled air. For the linkage component of the model, although the exhaled propofol concentration exhibited a delayed peak, the connection remained indirect. This is because the exhaled propofol concentration and the effect-site concentration did not achieve immediate equilibrium. The PK-PD model is essential for target-controlled infusion and even closed-loop drug administration. The establishment of the PK-PD model demonstrated that real-time analysis of exhaled air can directly guide the timing and dosage of fospropofol disodium administration, simplifying the titration of anesthesia depth and improving the safety of clinical anesthesia [33–35]. Moreover, upon awakening, no statistically significant difference was observed in the exhaled propofol concentration among the propofol groups, suggesting that exhaled propofol monitoring has potential for guiding extubation in beagles. Nevertheless, the exhaled propofol concentration threshold for awakening in beagles following the administration of fospropofol disodium increased with increasing dosage, potentially due to prolonged anesthesia and inconsistent baseline anesthetic effects of Zoletil.

This study also has several limitations. A primary limitation is that the PK-PD model was developed solely based on exhaled propofol concentrations. However, blood concentrations are generally more stable and reproducible than exhaled concentrations. Precise measurement of exhaled propofol concentrations requires stringent control of sampling procedures and the use of high-performance analytical instruments. In this study, experimental conditions were strictly standardized, and the VUV-TOF MS exhibited exceptionally high sensitivity, detecting propofol at levels as low as 0.04 ppbv. Additionally, the sampling lines, composed of polyether-ether-ketone tubing, were maintained at a constant temperature of 100 °C, which significantly reduced the loss of propofol gas sampling. Secondly, mixed exhaled air was analyzed instead of alveolar air due to the difficulties of collecting alveolar samples from beagles. On one hand, collecting mixed air is simpler and more feasible than alveolar gas, which has been investigated in many previous studies [19, 36–39]. During mechanical ventilation of anesthetized beagles, with fixed body position, respiratory rate, and tidal volume, a proportional relationship exists between the concentration of propofol in exhaled mixed air and alveolar air [40]. In exhalation analysis, employing reproducible and precise gas sampling methods is critically important. Further studies are needed to explore and optimize alveolar air collection techniques.

## Conclusions

This study is the first to develop a PK-PD model for exhaled propofol in beagles after fospropofol disodium administration. The PK profile was described by a two-compartment model with a first-order delay, and the PD profile was modeled using an inhibitory sigmoid $E_{max}$ model with an indirect connection model to capture the lag between BIS and exhaled propofol peaks. This study provides valuable insights and data support for future PK studies utilizing exhaled air analysis.

## Supplementary Information

The online version contains supplementary material available at https://doi.org/10.1186/s12917-025-04570-w.

Supplementary Material 1

**Acknowledgements**

The authors thank Professor. Jin Liu for guidance on the development of the PK-PD modeling.

**Author contributions**

Study conception and design: ZWS, LXX, CP Mass spectrometer design and modification: ZZJ, DYX Data collection: LXX, CP, LX Data analysis: LXX, CP, KY Drafting the manuscript: LXX, CP Revisions to the manuscript: ZWS, LXX, CP, ZZJ, DYX.

**Funding**

This study is supported by the Sichuan Province Science and Technology Support Program (2023YFS0136).

**Data availability**

No datasets were generated or analysed during the current study.

## Declarations

**Ethical approval**

The study was approved by the Animal Ethics Committee of West China Hospital, Sichuan University (20220420001), and all procedures were conducted in accordance with animal welfare regulations.

**Competing interests**

The authors declare no competing interests.

Received: 21 July 2024 / Accepted: 5 February 2025
Published online: 28 February 2025

**References**

1. Garnock-Jones KP, Scott LJ. Fospropofol Drugs. 2010;70:469–77.
2. Minto CF, Schnider TW. Contributions of PK/PD modeling to intravenous anesthesia. Clin Pharmacol ther. 2008;84:27–38.
3. Wu CM, Zhang WS, Liu J, Zhang WY, Ke BW. Efficacy and Safety of Fospropofol Disodium for Injection in General Anesthesia Induction for adult patients: a phase 3 trial. Front Pharmacol. 2021;12:687894.
4. Thomson AH, Elliott HL. Designing simple PK–PD studies in children. Pediatr Anesth. 2011;21:190–6.
5. De Cock RFW, Piana C, Krekels EHJ, et al. The role of population PK-PD modelling in paediatric clinical research. Eur J Clin Pharmacol. 2011;67:5–16.
6. Yu Y, Rüppel D, Weber W et al. PK/PD Approaches. Drug Discovery and Evaluation: Methods in Clinical Pharmacology. 2020: 1047-69.
7. Bruderer T, Gaisl T, Gaugg MT, et al. On-line analysis of exhaled breath: focus review. Chem Rev. 2019;119:10803–10.

8. Harrison GR, Critchley ADJ, Mayhew CA, et al. Real-time breath monitoring of propofol and its volatile metabolites during surgery using a novel mass spectrometric technique: a feasibility study. Br J Anaesth. 2003;91:797–9.
9. Boshier PR, Cushnir JR, Mistry V, et al. On-line, real time monitoring of exhaled trace gases by SIFT-MS in the perioperative setting: a feasibility study. Analyst. 2011;136:3233–7.
10. Jiang D, Chen C, Wang W, et al. Breath-by-breath measurement of intraoperative propofol by unidirectional anisole-assisted photoionization ion mobility spectrometry via real-time correction of humidity. Anal Chim Acta. 2021;1150:338223.
11. Li X, Chang P, Liu X, et al. A preclinical study on online monitoring of exhaled ciprofol concentration by the ultraviolet time-of-flight spectrometer and prediction of anesthesia depth in beagles. J Pharm Biomed Anal. 2023;235:115621.
12. Li X, Chang P, Liu X, et al. Calibration and validation of ultraviolet time-of-flight mass spectrometry for online measurement of exhaled ciprofol. Anal Methods. 2023;15:4179–86.
13. Li X, Chang P, Liu X, et al. Exhaled breath is found to be better than blood samples for determining propofol concentrations in the brain tissues of rats. J Breath Res. 2024;18:026004.
14. Maurer F, Walter L, Geiger M, et al. Calibration and validation of a MCC/IMS prototype for exhaled propofol online measurement. J Pharm Biomed Anal. 2017;145:293–7.
15. China National Food and Drug Administration. Guiding Principles for Registration Review of Animal Testing in Medical Device Studies. 2021; https://amr.hainan.gov.cn/himpa/HICDME/zdyz/ylqx/202109/t20210928_3067786.html
16. Henao-Guerrero PN, McMurphy R, Kukanich B, Hodgson DS. Effect of morphine on the bispectral index during isoflurane anesthesia in dogs. Vet Anaesth Analg. 2009;36:133–43.
17. Seddighi R, Geist A, Knych H, Sun X. The remifentanil infusion on sevoflurane minimum alveolar concentration-no movement (MACNM) and bispectral index in dogs. Vet Anaesth Analg. 2023;50:121–8.
18. March PA, Muir WW. Bispectral analysis of the electroencephalogram: a review of its development and use in anesthesia. Vet Anaesth Analg. 2005;32:241–55.
19. Chen X, Zhang XL, Liu L, et al. Gas chromatograph-surface acoustic wave for quick real- time assessment of blood/exhaled gas ratio of propofol in humans. Br J Anaesth. 2014;113:807–14.
20. Kreuer S, Hauschild A, Fink T, et al. Two different approaches for pharmacokinetic modeling of exhaled drug concentrations. Sci Rep. 2014;4:5423.
21. Ziaian D, Herrmann R, Kleiboemer K et al. Pharmacokinetic modeling of the transition of propofol from blood plasma to breathing gas. IEEE. 2014; pp: 1–5.
22. Anderson JC, Babb AL, Hlastala MP. Modeling soluble gas exchange in the airways and alveoli. Ann Biomed Eng. 2003;31:1402–22.
23. Anderson JC, Hlastala MP. Breath tests and airway gas exchange. Pulm Pharmacol Ther. 2007;20:112–7.
24. Eleveld DJ. Propofol PK-PD. Total Intravenous Anesthesia and Target Controlled Infusions: A Comprehensive Global Anthology. 2017; 191–208.
25. Liu L, Wang K, Yang Y, et al. Population pharmacokinetic/pharmacodynamic modeling and exposure-response analysis of ciprofol in the induction and maintenance of general anesthesia in patients undergoing elective surgery: a prospective dose optimization study. J Clin Anesth. 2024;92:111317.
26. Fechner J, Schwilden H, Schüttler J. Pharmacokinetics and pharmacodynamics of GPI 15715 or fospropofol (Aquavan injection) - a water-soluble propofol prodrug. Mod Anesthetics. 2008: 253–66.
27. D'Argenio DZ. Optimal sampling times for pharmacokinetic experiments. J Pharmacokinet Biopharm. 1981;9:739–56.
28. Aprea E, Morisco F, Biasioli F, et al. Analysis of breath by proton transfer reaction time of flight mass spectrometry in rats with steatohepatitis induced by high-fat diet. J Mass Spectrom. 2012;47:1098–103.
29. Liu S, Yao X, Tao J, et al. Population total and unbound pharmacokinetics and pharmacodynamics of ciprofol and M4 in subjects with various renal functions. Br J Clin Pharmacol. 2023;89:1139–51.
30. Cockshott ID, Douglas EJ, Plummer GF, et al. The pharmacokinetics of propofol in laboratory animals. Xenobiotica. 1992;22:369–75.
31. Grossherr M, Hengstenberg A, Dibbelt L, et al. Blood gas partition coefficient and pulmonary extraction ratio for propofol in goats and pigs. Xenobiotica. 2009;39:782–87.
32. Grossherr M, Varadarajan B, Dibbelt L, et al. Time course of ethanol and propofol exhalation after bolus injection using ion molecule reaction-mass spectrometry. Anal Bioanal Chem. 2011;401:2063–7.
33. Liu N, Chazot T, Genty A, et al. Titration of propofol for anesthetic induction and maintenance guided by the bispectral index: closed-loop versus manual control: a prospective, randomized, multicenter study. Anesthesiology. 2006;104:686–95.
34. Hornuss C, Wiepcke D, Praun S, et al. Time course of expiratory propofol after bolus injection as measured by ion molecule reaction mass spectrometry. Anal Bioanal Chem. 2012;403:555–61.
35. Eleveld DJ, Colin P, Absalom AR, Struys MMRF. Pharmacokinetic-pharmacodynamic model for propofol for broad application in anaesthesia and sedation. Br J Anaesth. 2018;121:519.
36. Lo'pez-Lorente CI, Awchi M, Sinues P, García-Go'mez: real-time pharmacokinetics via online analysis of exhaled breath. J Pharm Biomed Anal. 2021;205:114311.
37. Lawal O, Ahmed WM, Nijsen TME, et al. Exhaled breath analysis: a review of 'breath-taking' methods for off-line analysis. Metabolomics. 2017;13:1–16.
38. Heiderich S, Ghasemi T, Dennhardt N, et al. Correlation of exhaled propofol with Narcotrend index and calculated propofol plasma levels in children undergoing surgery under total intravenous anesthesia - an observational study. BMC Anesthesiol. 2021;21:161.
39. Braathen MR, Rimstad I, Dybvik T, et al. Online exhaled propofol monitoring in normal-weight and obese surgical patients. Acta Anaesthesiol Scand. 2022;66:598–605.
40. Li X, Chang P, Liu X, et al. Validation of a method for estimating pulmonary dead space in ventilated beagles to correct exhaled propofol concentration in mixed air. BMC Vet Res. 2025;21:9.


## Publisher's note